REPORT ON A STUDY OF GALAXY FORMATION IN SPH SIMULATIONS

P.B. TISSERA[1,2], R. DOMÍNGUEZ-TENREIRO[1], A. SÁIZ[1] and P. GOLDSCHMIDT[3]
[1] *Dpt. Física Teórica, UAM, Cantoblanco, 28049 Madrid, Spain*
[2] *IAFE, Casilla 67, Suc. 28, 1428 Buenos Aires, Argentina*
[3] *Imperial College of Science, Technology and Medicine, Blackett Laboratory, Prince Consort Road, London W37 2BZ, U.K.*

1. Introduction

The physical process that may be involved in the formation and evolution of galaxies, and their behaviour as a function of the redshift, can be of different natures. As a matter of fact, it is still unclear whether it is *nature* or *nurture* that really we should worry about (Ellis, 1997). During the last decade, a dramatic improvement in our understanding of the Universe has resulted from the development of important observational facilities. These new findings are helping astronomers to generate a more realistic picture of the evolution of structure and help to constrain models. However, how galaxies form and evolve remains an open question. Several complex processes acting on different scales are believed to be important.

Today, the most successful scenario for the formation of structure is hierarchical clustering (although several issues remain to be clarified). In standard cold dark matter models, a galactic object is made up mainly of dark matter and a small percentage of baryons (≤ 0.10; Burles and Tytler, 1998). Dark-matter haloes provide the potential well for the baryons to collapse, driving the global evolution of the structure. They acquire angular momentum by tidal torques during mergers and interactions. Within these haloes, baryons, initially in the form of gas, cool and collapse. It has been shown that, provided its angular momentum is conserved during this process (Fall and Efstathiou, 1980), the gas settles on to exponential discs. The accumulation of baryons in the central regions steepens the potential well of the system and this, in turn, modifies the dark-matter profiles. On this scale, the relative distribution of DM and baryons (i.e. which is dynamically dominating and which is determining the rotation curves of spiral galaxies) is an important issue in explaining several properties of galaxies. Because in this model the assembly of the structure is a hierarchical process, mergers and interactions play a critical role, affecting the properties of the matter in different ways. In this scenario, mergers

Astrophysics and Space Science **276:** 1087–1095, 2001.

and interaction rates increase with look-back time and it seems that this is actually being observed (Driver *et al.*, 1998).

One of the most relevant physical processes involved in galaxy formation is star formation. Stars are a main component in galaxies and their formation process could be tightly related to the properties of the galaxies we observe. The factors that trigger and regulate SF could be of different natures and interrelated among one another, so that the dynamics (i.e. collapse, mergers, interactions) can affect SF, but how SF proceeds (i.e. rate, IMF, supernova explosions) may also affect the dynamics of the galaxy (e.g. leading to the formation of stellar bulges). These facts make hydrodynamical cosmological simulations a powerful tool for studying galaxy formation.

In this paper, we intend to summarize comprehensively results on dark-matter haloes, cooling and collapse of baryons and SF, highlighting some of the effects that one may have on the others.

2. Numerical Experiments

We have followed the evolution of 64^3 particles in a periodic box of 10 Mpc ($H_0 = 50$ km s^{-1} Mpc^{-1}) using an SPH + AP3M code (Tissera, Lambas and Abadi, 1997). The initial conditions are consistent with a standard CDM cosmology, with $\Omega = 1$, $\Omega_b = 0.1$ and $\Lambda = 0$. The gravitational softening length is 3 kpc and the minimum allowed smoothing length is 1.5 kpc. All dark gas and star particles have the same mass, $M = 2.6 \times 10^8\ M_\odot$. The star formation algorithm used in these models transforms gas particles into stars if the gas is cold and dense ($\rho_{gas} > 7 \times 10^{-26}$ g cm^{-3}) and satisfies the Jeans instability criterion according to: $d\rho_{star}/dt = -\eta\rho_{gas}^{1.5}$ (Tissera *et al.*, 1997). No supernova explosion effects have been considered. In Table I we summarize the following characteristics: bias parameter, b, T_*, star formation efficiency, η, and whether it is a pure gravitational simulation (G) or a hydrodynamical one (H). Simulations I.1, I.2, I.3, II.1 and II.2 are analysed in Section 2, simulations I.2 and I.4 in Section 3 and simulations I.2, I.3 and III.1 by Domínguez-Tenreiro, Tissera and Sáiz (1998) and Tissera, Sáiz and Domínguez-Tenreiro (these proceedings).

Each set corresponds to different initial conditions. Simulations in each set share the initial conditions but have different star formation parameters. A pure gaseous run is indicated by $\eta = 0$. In all cases we analysed galaxy-like objects (GLOs) with more than 250 baryonic particles within their virial radii. The main baryonic objects within the haloes have been isolated using a friend-of-friends algorithm.

TABLE I

S	I.1	I.2	I.3	II.1	II.2	III.1
σ_8	0.40	0.40	0.40	0.60	0.60	0.67
η	0	0.01	0.1	0	0.01	0.01
$T*$	–	310^4	310^4	–	10^4	10^4

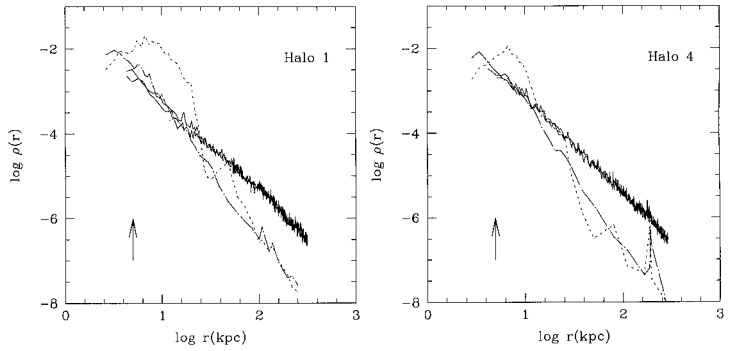

Figure 1. Density profiles of Halo 1 and Halo 4 in simulations I.2 and I.3: dark-matter density profiles (*solid lines*) and baryonic density profiles in I.2 (*dotted lines*) and I.3 (*dotted–long-dashed lines*).

3. Dark-Matter Distribution in Haloes

Dark matter (DM) is the principal component in the Universe and dominates gravitationally the evolution of the structure. In particular, the importance of understanding the formation and evolution of DM haloes depends on whether their statistical properties contain relevant information about cosmological parameters and the power spectrum of the initial density fluctuations (Tissera and Domínguez-Tenreiro, 1998). They also play a key role in galaxy formation and their properties (i.e. central concentration and distribution) are relevant to understanding the astrophysical properties of individual galaxies. Their formation and evolution may also be affected by baryons in a complex feedback process. In this section we analyse dark-matter haloes of the more massive objects in simulations I.1, I.2, I.3, II.1 and II.2. We compare the properties of haloes with and without baryons (see Section 2).

We found, in agreement with previous studies (e.g. Navarro, Frenk and White, 1996, NFW), that in the absence of baryons DM profiles follow the so-called NFW profile. But when baryons are included, the density profiles (DPs) are modified, becoming steeper at the centre ($\rho_{\rm DM} \propto r^{-2}$). The shapes of the haloes change from prolate to more oblate structures when baryons are included. A stronger increase in the total velocity dispersion of the DM is measured in the central regions of all haloes in SPH runs.

We found no systematic differences in the infall of baryons within $r_{\rm cross}$, defined as the radius that encloses the same amount of DM and baryons. However, a correlation between the maximum of the circular velocity curves and $r_{\rm cross}/r_{200}$ was found. This correlation seems to indicate that the distribution of baryons within the central region is different in different GLOs. Possible mechanisms that could produce this effect are mergers with substructure and the star formation history of the GLOs. Indeed, the values of $r_{\rm cross}/r_{200}$ seem to depend on the history of SF. If a large fraction of gas is transformed into stars at early times, the objects are less dominated by baryons at the centre because baryons have not had enough time to get that concentrated (by effects of dissipative processes). We clearly see this when comparing the properties of haloes in I.2 and I.3. These simulations share the same initial conditions but have different SF histories as already explained.

In Figure 1 we plot the DM DP and the baryonic DP for two typical haloes in I.2 (*dotted line*) and I.3 (*dot–dashed line*). A change in the star formation efficiency parameter has led to a different distribution of baryons in the central regions. It should be noted that the amount of baryons in the central region is the same in both cases, the difference is how they are distributed. In turn, this may affect the ongoing star formation.

4. Star Formation

In this section, we will analyse the SF histories of GLO simulations I.2, I.3 and III.1 (see Table I) and how mergers can affect them. In order to assess how the SF model works, we define a global star formation rate, SFR, as the ratio between the total mass of stars formed in the comoving box during an integration step and its length ($\Delta t = 1.4 \times 10^7$ yr, time bin length). Then, the cosmic star formation rate density is defined as $\rho_{SFR}(z) = \langle SFR(z) \rangle / V$, where $\langle SFR(z) \rangle$ is SFR averaged over 20 time bins centred at the formation redshift, z, of each star particle, and V is the comoving volume of the box at z.

In Figure 2 we plot $\rho_{SFR}(z)$ for I.2, I.3 and III.1, together with some estimates based on observations. $\rho_{SFR}(z)$ decreases by a factor of ≈ 12 from $z = 1$ to $z = 0$, independently of the simulation considered.

I.2 and I.3 start forming stars later in time than III.1, due to the lower normalization parameter and T_* used. Because of this, they also transformed a larger fraction of their mass into stars. We also included all published estimations of $\rho_{SFR}(z)$. The latest results show a flat $\rho_{SFR}(z)$ with z (i.e. Flores *et al.*, 1998). However, many uncertainties remain to be addressed from the observational side before a reliable global star formation history is available, and before a clean and accurate comparison with the outputs of simulations can be made. Renzini (1998) claims that approximately 30% of existing stars were formed at $z > 2$. Simulation III.1 shows a similar trend. It produces 30% of the total stellar mass at $z > 2$, and 55%

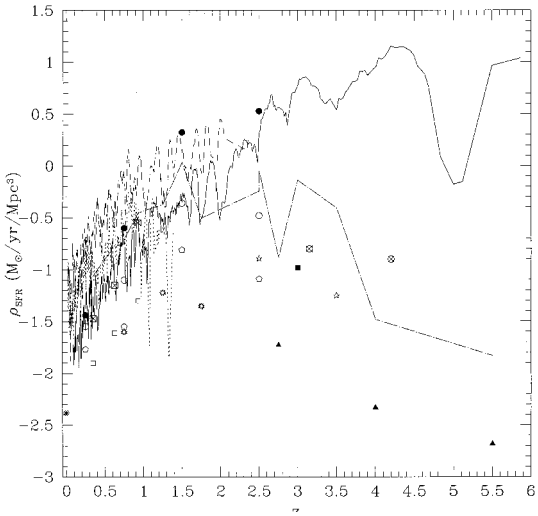

Figure 2. Cosmic star formation rate density, ρ_{SFR}, versus z for simulations I.1 (*dotted lines*), I.2 (*dashed lines*) and I.3 (*solid lines*). We also include observational values reported by Gallego *et al.* (1995) [*asterisk*], Madau *et al.* (1996) [*filled triangles*], Lilly *et al.* (1996) [*open squares*], Connolly *et al.* (1997) [*ten-arm stars*], Mobasher and Mazzei (1998) [*filled and open circles* and *open pentagons*], Sawicki, Lin and Yee (1997) [*open stars*], Hughes *et al.* (1998) [*filled square*], Flores *et al.* (1998) [*crossed open squares*] and Steidel *et al.* (1998) [*crossed open circles*]. The *dot–dashed line* shows the observation relation determined by all points (except Mobasher and Mazzei, 1998, and Gallego *et al.*, 1995) corrected by a factor of seven due to dust extinction.

at $1 < z < 2$. This continuous growth for $z > 2.5$ could be regulated by including feedback.

In order to study the SF history of each GLO, they are identified at their virial radii (r_{200}) at $z = 0$. Then, the evolution of the particles within r_{200} is followed back in time. In this way, we construct the merger tree of each GLO. The progenitor clump of a GLO is taken to be the most massive object identified at $z > 3$ in its merger tree. A merger will be counted each time the progenitor fuses with a satellite with more than 10% of its mass at the merger time. We compute the stellar mass formed in the progenitor as a function of z and define its $\langle SFR \rangle$ history, as previously described. In all cases, there is an increase of $\langle SFR \rangle$ related to merger events (Figure 3), from the time the satellite enters the virial region of the progenitor (arrows pointing up, beginning of the orbital decay period), up to the fusion of the baryonic cores (arrows pointing down).

The cooling and collapse of gas in quiescent phases of evolution drive an ambient star formation rate, estimated to be $\leq 3\ M_\odot\ \mathrm{yr}^{-1}$. Stellar formation bursts are superposed on the ambient star formation. We focus on the analysis of those bursts occuring within merger events. Its duration, τ_{burst}, its local maximum SFR, σ_{star}, and the total amount of stellar mass formed during the burst, M_{burst}, can be estimated (see Tissera et al., 2000). For III.1, $\langle \tau_{\mathrm{burst}} \rangle$ and $\langle M_{\mathrm{burst}} \rangle$ are consistent

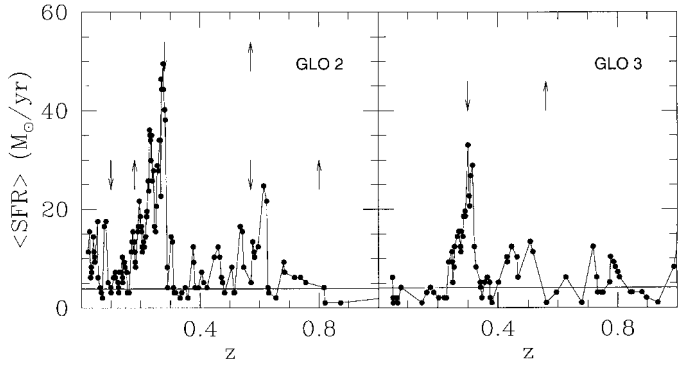

Figure 3. Star formation rate history of four galaxy-like objects analysed in simulation I.3. The *horizontal solid line* represents the ambient star formation rate, $\sigma_{\rm min}$, for each object.

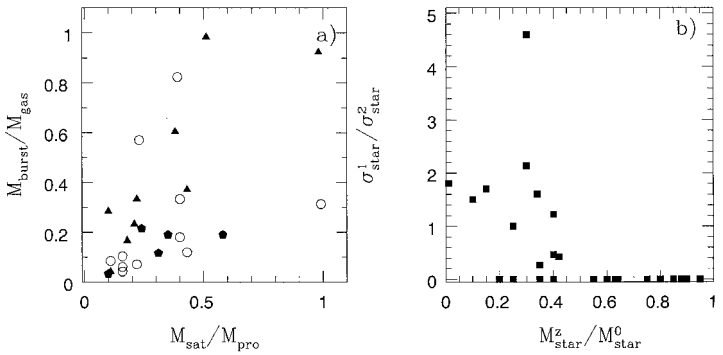

Figure 4. The fraction of gas converted into stars in a star formation burst, $M_{\rm burst}/M_{\rm gas}$, versus the relative masses of the colliding objects, $M_{\rm sat}/M_{\rm pro}$ (*left*); ratio between the strengths of the double star bursts ($\sigma^1_{\rm star}/\sigma^2_{\rm star}$) and the fraction of stars already formed in the progenitor GLO ($M^z_{\rm star}/M^0_{\rm star}$) at the z of the merger ($z_1 > z_2$). Single bursts have been assigned $\sigma^1_{\rm star}/\sigma^2_{\rm star} = 0$ (*right*).

with observed values inferred from some starburst galaxies at high z (Kennicutt, 1988, and references therein). The other simulations produce higher ones.

To try to establish which factors determine the properties of the bursts, we have measured $M_{\rm pro}$, $M_{\rm sat}$ (virial masses of the progenitor and satellite before the latter enters the virial radius of the progenitor), $M_{\rm gas}$ and $M_{\rm bar}$ (the total gas mass and the total baryonic mass) of the progenitor and satellite together within r_{200} before the merger. These are measures of the total amount of gas and baryons available before the merger event. We also estimate, $M^{\rm m}_{\rm gas}$, the mass of the main baryonic clump before the merger. We only found a correlation signal between the burst efficiency, $M_{\rm burst}/M_{\rm gas}$, and $M_{\rm sat}/M_{\rm pro}$, indicating that more massive mergers induce more efficient transformations of gas into stars (Figure 4, *left*).

An important parameter describing the internal structure of baryonic merging clumps is the mass of their central stellar bulge-like concentrations, if present.

Several authors have observed that when bulges are missing, strong gas inflows can follow disc bar instabilities, during the orbital decay phase in merger events. These could, in turn, trigger stellar bursts. If this is the case, the whole merger would cause a star formation burst with two peaks, the first one caused by disc instability during the orbital decay phase and the second by the fusion of the baryonic clumps. Given our numerical resolution, a detailed analysis of the internal structure is not possible, but, because the SF algorithm is mainly based on a density criterion condition, the formation of a stellar bulge can be directly linked to the fraction of gas that has been transformed into stars. We define $M^{z}_{\rm star}$, the mass of stars in the progenitor at redshift z and $M^{z}_{\rm star}/M^{z=0}_{\rm star}$, the fraction of stars in the final object already formed at the z of the merger, as our indicator of the presence of a well formed stellar bulge. A clear relation has been found between the relative strengths of the two peaks and $M^{z}_{\rm star}/M^{z=0}_{\rm star}$ for a given merger. Those progenitors with $M^{z}_{\rm star}/M^{z=0}_{\rm star} < 0.4$ are more susceptible to experience inflow events because they have no important stellar bulge at the merger time. Those progenitors with $M^{z}_{\rm star}/M^{z=0}_{\rm star} > 0.4$ are more stable (see Tissera, Sáiz and Domínguez-Tenreiro, these proceedings). They are not found to be involved in double peak bursts. This clear correlation shows that the physics has been globally well described. A trend to have larger burst efficiency, $M_{\rm burst}/M_{\rm gas}$, in more unstable systems was found, implying that stellar bursts induced by tidal fields during the orbital decay phase may be more efficient.

5. Discussion

It has been previously shown (Fall and Efstathiou, 1980) that gaseous discs with exponential surface density profiles and observational counterparts can be formed if the gas cools and collapses conserving its specific angular momentum. In Domínguez-Tenreiro, Sáiz and Tissera (this proceeding) and Tissera, Sáiz and Domínguez-Tenreiro (these proceedings), we discuss the formation of disc-like structures in hierarchical clustering models. It has also been proved that, within the context of hierarchical clustering, the hypothesis of angular momentum conservation is very difficult to maintain. During mergers and interactions angular momentum is transferred from the gaseous component to the dissipationaless component (e.g. Barnes, 1992; Navarro and Steinmetz, 1997; Domínguez-Tenreiro *et al.*, 1998). So that when mergers are complete the gas has lost most of its j and is concentrated in a very small disc. A mechanism that also affects the formation of discs is SF. How SF proceeds may be relevant to the morphology of the final object. If the gas is quickly exhausted at high z, no gaseous remnant will be left to regenerate discs at a later stage. However, because the structure is assembled through mergers, the SF is also affected by them. The output of these violent phases critically depends on the availability of gas to regenerate a disc structure on one hand, and on the structural stability of the objects involved in the event on the other. Concerning stability, cold thin discs are known to be violently unstable against the bar mode (Domínguez-

Tenreiro *et al.*, 1998, and references therein). Massive haloes can stabilize discs, but not every halo is able to stabilize the exponential disc that would form in the quiescent phases of evolution. In these cases, a central compact bulge is needed to ensure stability, otherwise a bar instability could easily be triggered by interactions and mergers, followed by strong gas inflows. These gas inflows, in turn, can trigger star formation. As was shown in Section 4, we found that GLOs lacking major stellar mass concentration at the centre experience double star bursts. These results agree with those found by Domínguez-Tenreiro *et al.* (1998), which detect these strong inflows in unstable systems.

Hence, how SF is regulated or self-regulates at different z is a key point for understanding galaxy formation. And this remains an open question, since the physical processes that might be involved are of diverse natures and their effects may vary with redshift.

References

Athanassoula, E. and Sellwood, J.: 1986, *Mon. Not. R. Astron. Soc.* **221**, 213.
Barnes, J.E.: 1992, *Astrophys. J.* **341**, 425.
Barnes, J.E. and Hernquist, L.: 1991, *Astrophys. J. Lett.* **370**, L65.
Barnes, J.E. and Hernquist, L.: 1992, *Annu. Rev. Astron. Astrophys.* **30**, 705.
Barnes, J.E. and Hernquist, L.: 1996, *Astrophys. J.* **471**, 115.
Binney, J. and Tremaine, S.: 1987, *Galactic Dynamics*, Princeton Univ. Press, Princeton.
Burles, S. and Tytler, D.: 1998, *Astrophys. J.* **499**, 699.
Chapelon, S., Contini, T. and Davoust, E.: 2000, *Astron. Astrophys.*, submitted.
Connolly, A.J., *et al.*: 1997, *Astrophys. J.* **486**, 11.
Courteau, S.: 1997, in: D. Block and M. Greenber (eds.), *Morphology and Dust Content in Spiral Galaxies*, Kluwer, Dordrecht.
Dalcanton, J.J., Spergel, D.N. and Summers, F.J.: 1997, *Astrophys. J.* **482**, 659.
Domínguez-Tenreiro, R., Tissera, P.B. and Sáiz, A.: 1998, *Astrophys. J. Lett.* **508**, L123.
Driver, S.P., Fernandez-Soto, A., Couch, W.J., Odewahn, S.C., Windhorst, R.A., Lanzetta, K. and Yahil, K.: 1998, *Astrophys. J. Lett.* **498**, 93L.
Ellis, R.S.: 1997. in: K. Sato (ed.), Proc. IAU Symp. **183**, *Cosmological Parameters and Evolution of the Universe*, Kluwer, Dordrecht.
Fall, S.M. and Efstathiou, G.: 1980, *Mon. Not. R. Astron. Soc.* **193**, 189.
Flores, H., *et al.*: 1998, *Astrophys. J.* **517**, 148.
Gallego, J., Zamorano, J., Arágon-Salamanca, A. and Rego, M.: 1995, *Astrophys. J. Lett.* **455**, L1.
Hughes, D., *et al.*: 1998, *Nature* **394**, 241.
Kennicutt, R. Jr.: 1998, preprint.
Lilly, S., Le Fevre, O., Hammer, F. and Crampton, D.: 1996, *Astrophys. J.* **460**, 1.
Madau, M.P., Ferguson, H.C., Dickinson, M.E., Giavalisco, M., Steidel, C.C. and Fruchter, A.: 1996, *Mon. Not. R. Astron. Soc.* **283**, 1388.
Mihos, J.C. and Hernquist, L.: 1994, *Astrophys. J. Lett.* **425**, L13.
Mihos, J.C. and Hernquist, L.: 1996, *Astrophys. J.* **464**, 641.
Mo, H.J., Mao, S. and White, S.D.M.: 1998, *Mon. Not. R. Astron. Soc.* **295**, 319.
Mobasher, B. and Mazzei, P.: 1998, in: R. Weymann *et al.* (eds.), ASP Conf. Ser. **191**, *Photometric Redshifts and the Detection of High Redshift Galaxies*, ASP, San Francisco, p. 37.
Navarro, J.F. and Steinmetz, M.: 1997, *Astrophys. J.* **438**, 13.

Navarro, J.F., Frenck, C. and White, S.D.M.: 1996, *Astrophys. J.* **462**, 563.
Renzini, A.: 1998, astro-ph/9810304 (not yet published).
Sawicki, M., Lin, H. and Yee, H.K.: 1997, *Astron. J.* **113**, 1.
Steidel, C.C., Adelberger, K.L., Giavalisco, M., Dickinson, M. and Pettini, M.: 1998, *Astrophys. J.* **519**, 1.
Steinmetz, M. and Navarro, J.F.: 1998, *Astrophys. J.* **513**, 555.
Steinmetz, M. and White, S.D.M.: 1997, *Mon. Not. R. Astron. Soc.* **289**, 545.
Tissera, P.B.: 2000, *ApJ* **534**, 636.
Tissera, P.B. and Domínguez-Tenreiro, R.: 1998, *Mon. Not. R. Astron. Soc.* **297**, 177.
Tissera, P.B., Lambas, D.G. and Abadi, M.G.: 1997, *Mon. Not. R. Astron. Soc.* **286**, 384.
Toomre, A.: 1981, in: S.M. Fall and D. Lynden-Bell (eds.), *The Structure and Evolution of Normal Galaxies*, Cambridge Univ. Press, Cambridge, p. 111.
Weil, M.L., Eke, V.R. and Efstathiou, G.: 1998, *Mon. Not. R. Astron. Soc.* **300**, 773.